Visualization of Sugar Content in the Flesh of a Melon by Near-Infrared Imaging

Junichi Sugiyama†

National Food Research Institute, 2-1-2 Kan-nondai, Tsukuba, Ibaraki 305-8642, Japan

The relationship between the sugar content and absorption spectra was investigated using a near-infrared (NIR) spectrometer to visualize the sugar content of a melon. The absorbance at 676 nm, which is close to the absorption band of chlorophyll, exhibited a strong inverse correlation with the sugar content. A high-resolution cooled charged couple device imaging camera fitted with a band-pass filter of 676 nm was used to capture the spectral absorption image. The calibration method used for converting the absorbance values on the image into the °Brix sugar content was developed in accordance with NIR spectroscopy techniques. When this method was applied to each pixel of the absorption image, a color distribution map of the sugar content was constructed.

Keywords: *Melon; sugar content; near-infrared; NIR; imaging; CCD camera*

INTRODUCTION

In Japan, automated sweetness sorting machines for peaches, apples, and melons based on near-infrared (NIR) spectroscopy techniques have been developed and are now in use in more than 1000 packing houses (Kawano, 1994). However, parts of a fruit sorted by the machine as sweet may sometimes taste insipid because of an uneven distribution of the sugar content. Visualization of the sugar content of a melon is expected to be useful not only for evaluation of its quality but also for physiological analysis of the ripeness of a melon. There have been several attempts at obtaining a distribution map of the constituents of agricultural produce (Robert et al., 1991, 1992; Bertrand et al., 1996; Taylor and McClure, 1989). However, a quantitatively labeled distribution map has not yet been obtained.

On the other hand, recently, device and personal computer (PC) technology have advanced greatly. Cooled charged couple device (CCD) imaging cameras with a wide dynamic range have been introduced and make quantitative measurements possible. Modern PCs can easily accept and/or process a large volume of data. Taking advantage of these, the conventional NIR spectroscopy technique, which is a technique for point measurement, could be extended to two-dimensional measurements. The objective of this research is to develop a technique for visualization of the sugar content of a melon by applying NIR spectroscopy to each pixel in an image.

MATERIALS AND METHODS

NIR Spectroscopy. To determine the wavelength, which has a high correlation with sugar content, spectra between 400 and 1100 nm of the flesh of a melon were analyzed using a NIR spectrometer (NIRS 6500, NIR Systems, Silver Spring, MD). This wavelength range covers the spectral range of the CCD camera used for our imaging application. A cylindrical sample with a diameter of 20 mm was extracted from the equator of the melon by a stainless steel cylinder with a knife edge at one end (Figure 1). A spectrum of the sample's inner surface was obtained using a fiber-type detector with an interactance mode (Kawano et al., 1992). The wavelength interval was 2 nm, and the number of scans was 50. The measured portion was then cut into a 2-mm-thick slice by a kitchen knife and squeezed with a portable garlic crusher to measure the °Brix sugar content using a digital refractometer (PR-100, ATAGO, Yorii, Saitama, Japan). The measurements of the spectrum and the sugar content were repeated similarly at various depths of the melon.

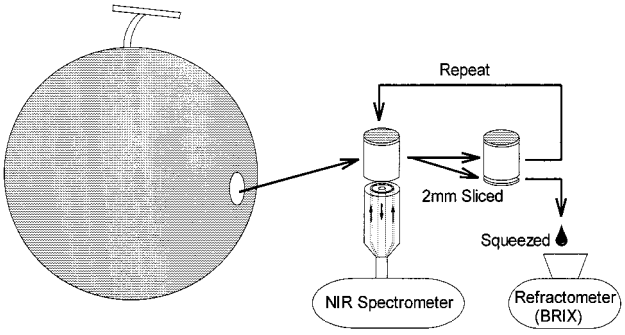

Figure 1. Sample preparation for measurements of NIR spectra and the sugar content.

Samples. Three ripeness stages (unripe, mature, and fully mature) of Andes melons harvested in Tsuruoka, Yamagata Prefecture, Japan, in 1998 were analyzed. Unripe melons were harvested 6 days earlier, and fully mature ones 5 days later than the mature melons. The mature melons were harvested 55 days after pollination. Two melons at each stage, that is, a total of six melons, were investigated. There were cracks on the bottom of the fully mature melons because of overripening. Each sample was sent to our laboratory the day after the harvest using a special delivery service. Experiments were carried out in a dark room at 25 °C.

Instrumentation. Figure 3 shows the configuration of the imaging apparatus used to obtain the spectroscopic images. Although a monochrome CCD camera normally has an 8-bit (256 steps) A/D resolution, we adopted a cooled CCD camera (CV-04II, Mutoh Industries Ltd., Tokyo, Japan) with a 16-bit (65536 steps) A/D resolution. The advantage of the high A/D resolution in this research is that each pixel can function as a detector of the NIR spectrometer for quantitative analysis. The CCD camera has a linear intensity characteristic ($\gamma = 1$) and no antiblooming gate for quantitative analysis. To decrease

† E-mail sugiyama@affrc.go.jp; fax +81-298-38-7996.

10.1021/jf981079i CCC: $18.00
Published on Web 06/17/1999

the electrical dark current noise of the CCD camera, both double-stage thermoelectric cooling and water cooling were utilized. A camera lens (FD28 mm F3.5 S.C., Canon, Tokyo, Japan) with an interference filter (J43192, Edmond Scientific, Tokyo, Japan) was installed through the camera adapter (Koueisya, Kawagoe, Saitama, Japan). The interference filter had band-pass characteristics of 676 nm at the central wavelength, which was determined in a preliminary NIR spectroscopic experiment (see Results and Discussion), and 10 nm at half-bandwidth. The illuminator (LA-150S, Hayashi Watch-Works, Tokyo, Japan) had a tungsten−halogen bulb driven by direct current to reduce optical noise. The source light was introduced into two fiber-optic probes, illuminating a sample from two different positions so as not to create any shadows or direct reflection. A sample was placed perpendicularly on the quartz glass, maintaining a constant focal distance between the CCD camera and the sample (Figure 3). The sample was supported by the moving wall covered with a black antireflection velvet sheet.

Image of Half-Cut Melon for Sugar Distribution Map. Each melon (six in total) was cut vertically in half with a kitchen knife. Spectroscopic images of the surface of a half-cut melon at 676 nm were taken with an aperture of 16 (F16) and an exposure period of 0.5 s. The cooling temperature of the CCD camera was −15 °C. The size of the image was 768 × 512 pixels. After a vertical image of the half-cut melon had been obtained, the melon was cut in a horizontal plane, and a horizontal image of the quarter-cut melon was captured under the same condition as described above.

Partial Image for Sugar Content Calibration. After the aforementioned images had been obtained, two cylindrical samples with a diameter of 20 mm were extracted from the equator of the same melon. In the same manner as in the NIR spectroscopic experiment (Figure 1), an image of the surface was taken at 676 nm using the CCD camera under the same condition as for the half-cut melon described previously. A 2-mm-thick slice was then cut off and squeezed for the measurement of sugar content. These procedures were repeated until the rind appeared.

Noise Corrections. Images acquired using a CCD camera include (i) thermal noise due to dark current thermal electrons, (ii) bias signals to offset the CCD slightly above zero A/D counts, (iii) sensitivity variations from pixel to pixel on the CCD, and (iv) lighting variations on the sample's surface. To compensate for the above, the following noise corrections (SBIG, 1998; Morita et al., 1992; Fukushima, 1996) were carried out.

$$\text{processed image} = \frac{\text{raw image} - \text{dark frame}}{\text{flat field} - \text{dark frame of flat field}} \times M \quad (1)$$

In eq 1, the dark frame is the image acquired under the same condition as the raw image except for the absence of lighting. Subtracting it from the raw image allows corrections for (i) thermal noise and (ii) bias signals. On the other hand, the flat field is obtained by taking an exposure of a uniformly lit "flat field" such as a Teflon board. After the dark frame of the flat field has been subtracted, in the same way as the numerator, the ratio between the two images is compensated for the effect of (iii) sensitivity variations and (iv) lighting variations. M is the intensity value averaged over all pixels of the flat field after dark frame subtraction (= denominator in eq 1). The multiplier M restores the ratio of the images to the image intensity level.

All of these image processes were carried out using software (CCD Master, Mutoh Industries Ltd., Tokyo, Japan) compatible with the CCD camera.

RESULTS AND DISCUSSION

Wavelength Selection by NIR Spectroscopy. Figure 2 shows the simple correlation coefficient calculated by a standard regression model with no data pretreatment between the absorbance at each wavelength and the sugar content. Each line was calculated from 22 slices made from 2 cylindrical samples that were extracted from a melon. It is clear that the wavelength of 676 nm exhibits the maximum absolute correlation, although it is inversely correlated with the sugar content for both the Andes and Earl's varieties of melon. Because of the inverse correlation, it seems that 676 nm is not a direct absorption band of sugar but a wavelength of secondary correlation (Osborne and Feam, 1986) with a component inversely proportional to the sugar content. It is actually close to the absorption band of chlorophyll (Stephan et al., 1994; Watada et al., 1976), and there are some implications for other produce (Izumi et al., 1990; Morita et al., 1992). Although we can take advantage of the fact that absorbance at 676 nm is inversely correlated with the sugar content for its visualization, the interpretation of 676 nm is also important in terms of the physiological aspects and must be further studied.

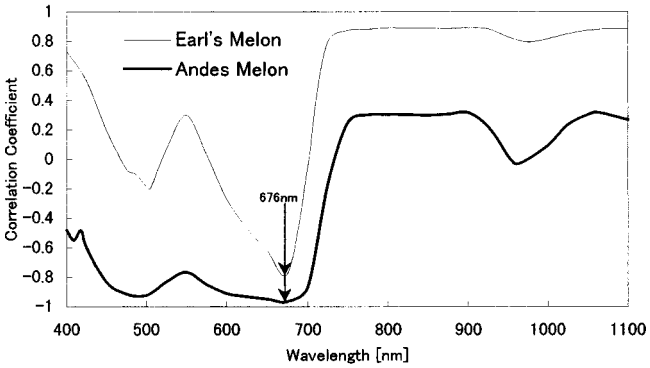

Figure 2. Correlation coefficients at each wavelength between the absorbance and the °Brix sugar content.

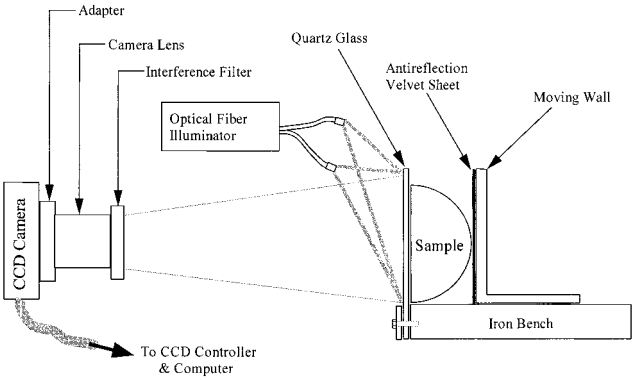

Figure 3. Configuration of an imaging apparatus.

Conversion from Intensity into Sugar Content. Each pixel of the image processed using eq 1 has 16 bits, that is, 65536 levels of intensity. The method for converting the intensity into sugar content on an image data was developed in accordance with NIR spectroscopy. On the basis of the fact that the functional group of chemical compounds responds to near-infrared radiation, NIR spectroscopy can measure the amount of a specific constituent from its absorbance at several wavelengths (Osborne and Feam, 1986). Absorbance A can be defined as

$$A = \log(Is/I) \quad (2)$$

where Is is the intensity of reflection of a white standard board and I is the intensity of reflection of the sample.

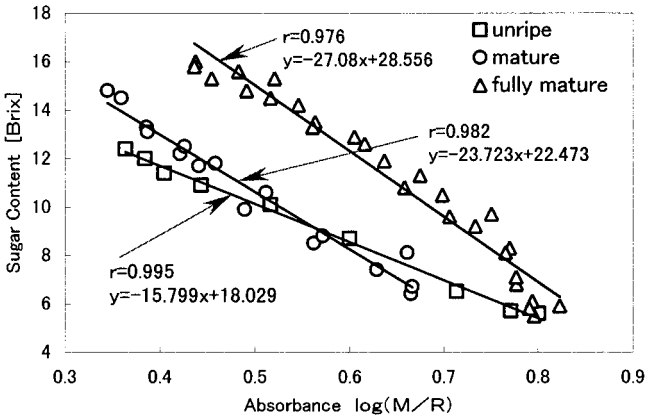

Figure 4. Calibration curves between the sugar content and the absorbance at 676 nm by the imaging system.

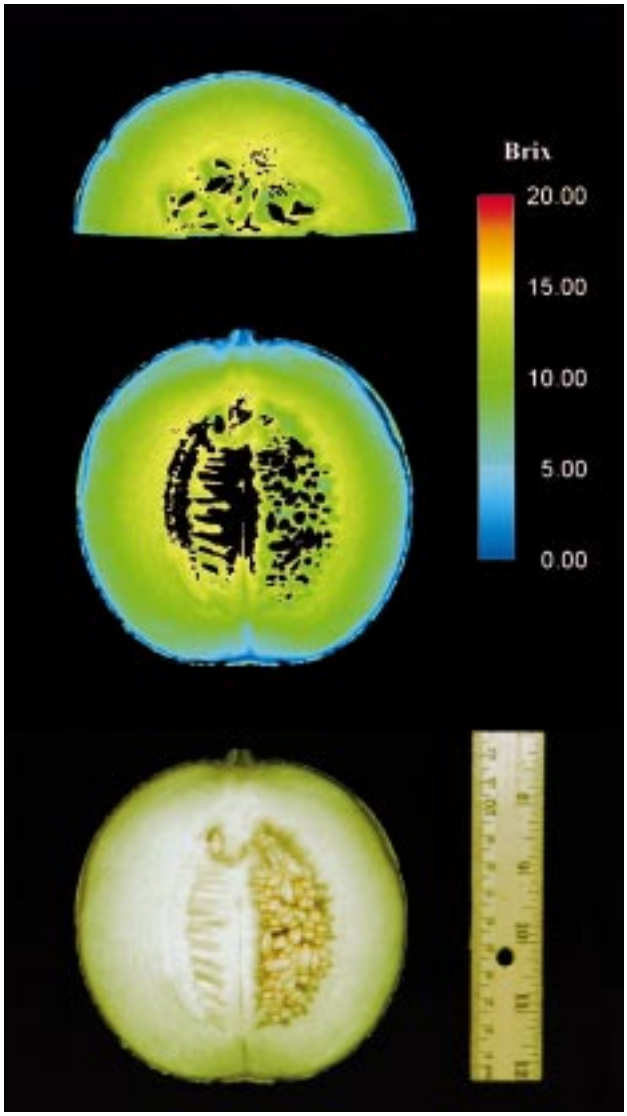

Figure 5. Sugar distribution map of an unripe melon.

Because *Is* and *I* correspond to the denominator and the numerator in the first term of eq 1, respectively, eqs 3 and 4 are introduced.

$$Is = \text{flat field} - \text{dark frame of flat field} \quad (3)$$

$$I = \text{raw image} - \text{dark frame} \quad (4)$$

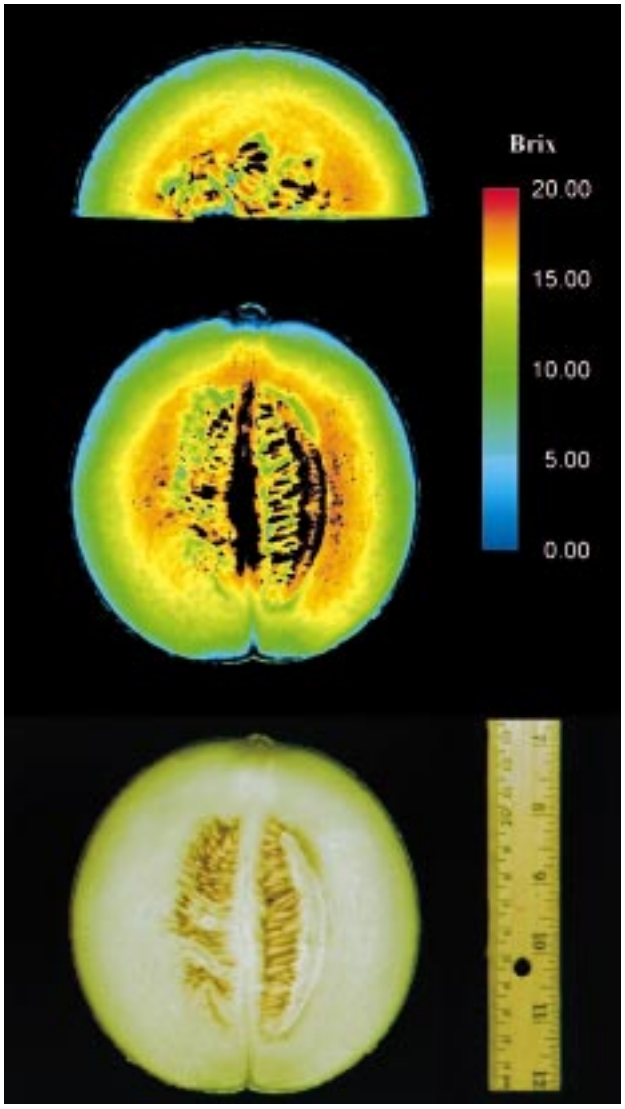

Figure 6. Sugar distribution map of a mature melon.

Considering eqs 1−4, absorbance *A* in the spectroscopic image can be expressed as follows.

$$\begin{aligned} A &= \log(Is/I) \\ &= \log(M/\text{processed image}) \\ &= \log(M/R) \end{aligned} \quad (5)$$

R is the intensity of the reflection of each pixel in a processed image, and *M* is the average intensity of reflection of the flat field.

On the other hand, the NIR spectroscopic experiment indicated that the absorbance at 676 nm was correlated with the sugar content. We confirmed the same relationship in the image system of this experiment using the following procedure: (i) calculation of the average intensity of a partial image of 20 mm diameter; (ii) conversion of the average intensity into absorbance using eq 5; (iii) plotting the relationship between the absorbance and sugar content for each partial image. A total of six melons, two for each stage of ripeness, were analyzed, and the representative results for unripe, mature, and fully mature melons are shown in Figure 4. The number of symbols in Figure 4 indicates the number of the sliced samples subjected to measurements of the absorbance and sugar content. Each

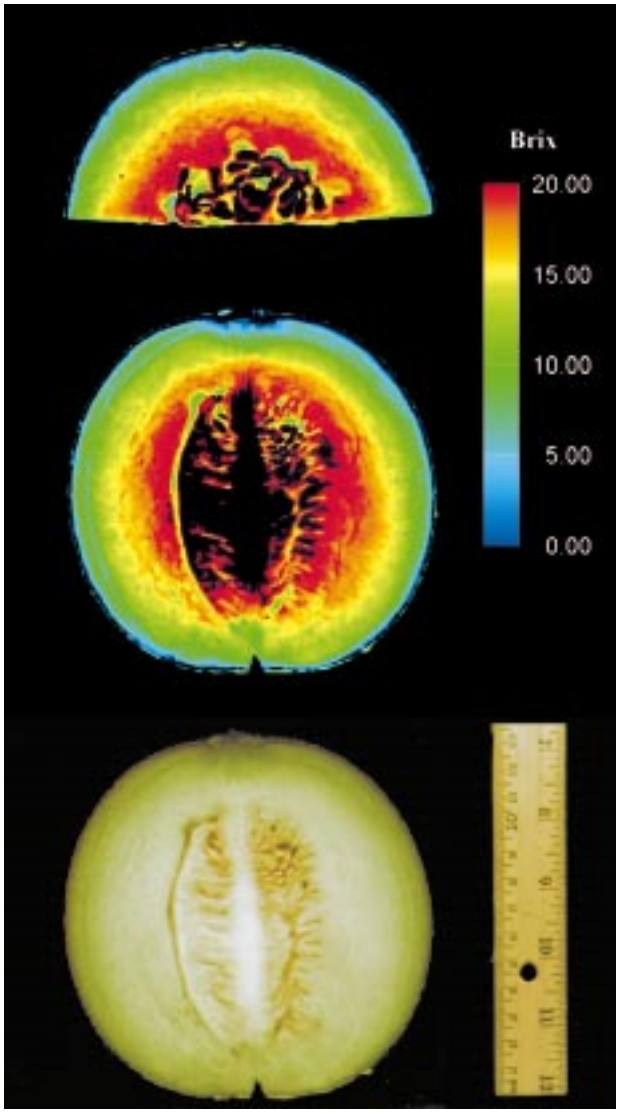

Figure 7. Sugar distribution map of a fully mature melon.

calibration curve is slightly different from the others because the light condition had been adjusted for each sample to avoid direct reflection (glittering) on rugged portions. This adjustment changed the lighting intensity level, which is not corrected by eq 1, and subsequently affected the calibration curves. However, it was confirmed that the image system can reveal the sugar content using the calibration curves for each sample.

Visualization of Sugar Distribution. The image of a half-cut melon for drawing a sugar distribution map was corrected for noise using eq 1. The processed image was converted into an absorbance image using eq 5. An image of sugar content was then calculated by applying the calibration curve to each pixel of the absorbance image. These actual procedures, from retrieval of the processed image to saving the sugar content image, were carried out using our own program written in Visual Basic (Microsoft, Redmond, WA). Finally, the sugar content image was visualized with a linear color scale by visualization software (AVS/Express Viz, Advanced Visual Systems, Waltham, MA). Figures 5, 6, and 7 show the results of visualization of the sugar content corresponding to unripe, mature, and fully mature melons, respectively. Because the measurements were carried out just after the harvest, the flesh of each melon was sufficiently hard and it was actually difficult to tell the differences in sugar content by the naked eye. However, as a result of the visualization, the sugar content at each stage of ripeness was clarified. In particular, in Figures 6 and 7, the distribution of the sugar content varies among different parts of the melon, indicating the importance of the part of the fruit sampled in the conventional measurement of the sugar content with a refractometer. In addition, as shown in Figure 6, the upper part had a higher sugar content than the bottom part. These results suggest that the visualization technique by NIR imaging could become a useful new method for quality evaluation of melons. Moreover, there is a good possibility that applying several wavelengths for the calibration curve could allow visualization of many more constituents of other agricultural products.

ACKNOWLEDGMENT

I gratefully thank Dr. Sumio Kawano for running the NIR spectrometer.

LITERATURE CITED

Bertrand, D.; Robert, P.; Novales, B.; Devaux, M. Chemometrics of multichannel imaging. In *Near Infrared Spectroscopy: The Future Waves*; Davies, A. M. C., Williams, P., Eds.; NIR Publications: Chichester, U.K., 1996; pp 174−178.

Fukushima, H. Basics of Image Analysis. In *Reikyaku CCD nyuumon*; Seibundou Sinkousha: Tokyo, Japan, 1996.

Izumi, H.; Ito, T.; Yoshida, Y. Seasonal changes in ascorbic acid, sugar and chlorophyll contents in Sun and shade leaves of Satsuma mandarin and their interrelationships. *J. Jpn. Soc. Hortic. Sci.* **1990**, *59*, 389−397.

Kawano, S. Present condition of nondestructive quality evaluation of fruits and vegetables in Japan. *Jpn. Agric. Res. Q.* **1994**, *28*, 212−216.

Kawano, S.; Watanabe, H.; Iwamoto, M. Determination of sugar content in intact peaches by near-infrared spectroscopy with fiber optics in interactance mode. *J. Jpn. Soc. Hortic. Sci.* **1992**, *61*, 445−451.

Morita, K.; Shiga, T.; Taharazako, S. Evaluation of change in quality of ripening bananas using light reflectance technique. *Mem. Fac. Agric. Kagoshima Univ.* **1992**, *28*, 125−134.

Nussberger, S.; Dekker, J. P.; Kuhlbrandt, W.; van Bolhuis, B. M.; van Grondelle, R.; van Amerongen, H. Spectroscopic characterization of three different monomeric forms of the main chlorophyll a/b binding protein from chloroplast membranes. *Biochmistry* **1994**, *33*, 14775−14783.

Osborne, B. G.; Feam, T. Near-infrared data handling and calibration by multiple linear regression. In *Near Infrared Spectroscopy in Food Analysis*; Longman Scientific & Technical: Harlow, U.K., 1986.

Robert, P.; Devaux, M. F.; Bertrand, D. Near-infrared video image analysis. *Sci. Aliments* **1991**, *11*, 565−574.

Robert, P.; Bertrand, D.; Devaux, M. F.; Sire, A. Identification of chemical sonstituents by multivariate near-infrared spectral imaging. *Anal. Chem.* **1992**, *24*, 664−667.

SBIG. *Product Catalog*; SBIG Astronomical Instruments: Santa Barbara, CA, 1998.

Taylor, S. K.; McClure, W. F. NIR imaging spectroscopy: measuring the distribution of chemical components. In *Proceedings of the 2nd International NIRS Conference*; Iwamoto, K., Kawano, S., Eds.; Korin: Tokyo, Japan, 1989; pp 393−404.

Watada, A. E.; Norris, K. H.; Worthington, J. T.; Massie, D. R. Estimation of chlorophyll and carotenoid contents of whole tomato by light absorbance technique. *J. Food Sci.* **1976**, *41*, 329−332.

Received for review September 21, 1998. Revised manuscript received March 24, 1999. Accepted April 2, 1999.

JF981079I